Photovoltaic Characterization Under Artificial Low Irradiance Conditions Using Reference Solar Cells

Behrang H. Hamadani and Mark B. Campanelli

***Abstract*—Due to the rapidly growing interest in energy harvesting from indoor ambient lighting for the powering of Internet-of-things devices, accurate methods for measurements of the current versus voltage characteristics of light-harvesting solar photovoltaic devices must be established and disseminated. A key requirement when conducting such characterizations is to create and measure the irradiance from the test light, whose spectral output approximates the profile of some agreed-upon standard reference. The current methods for measuring the irradiance from indoor ambient lighting (e.g., illuminance meters) can yield unacceptable discrepancies in measurements from one lab to another. Here, we take the first steps in establishing a more accurate alternative, i.e., using a calibrated reference solar cell to measure the total irradiance of the test light when establishing the test light level, and then, once set, while collecting the characterization data for the test specimen. The method involves establishing multiple reference indoor lighting spectra that meet desired illuminance requirements, while also offering precise spectral irradiance profiles. Regardless of whether these proposed spectra are formally adopted, the test method is available and useful. The proposed approach facilitates interlab measurements, allows for a way to calculate an accurate power conversion efficiency, and establishes a dialogue between National Metrology Institutes to begin the process of drafting standards for solar cell testing under conditions that are significantly different than the well-established standard reporting condition used for rating solar modules that are deployed outdoors.**

***Index Terms*—Ambient light, current versus voltage measurements, energy harvesting, indoor light, irradiance, photovoltaics.**

I. Introduction

In RECENT years, there has been a growing interest in measurements and characterization of solar cells under artificial or natural low light conditions. These efforts have been especially motivated by the need to harvest and repurpose a small portion of ambient light energy in office spaces and homes for powering a variety of electronic devices, especially Internet-of-things smart sensors [1]–[5]. The amount of available ambient light energy and the efficiency of the various photovoltaic (PV) technologies at harvesting this energy have been a subject of much work. Theoretical modeling has shown that for typical visible-light-spectrum sources, such as white light emitting diodes (LEDs) and fluorescent tube lighting, the highest power conversion efficiencies (PCE) are expected for PV materials with band gap energies of 1.8 to 2 eV [6], [7]. A variety of organic or hybrid photovoltaic materials [8]–[13], thin film devices [14], and some inorganic III–V materials such as GaInP and GaAs devices [15]–[17] are well suited for energy harvesting under these lighting conditions. By comparison, the most widely used commercial PV material, Silicon (Si), performs relatively poorly under indoor ambient light conditions [18]–[20].

While the actual task of measuring the current versus voltage (*I*–*V*) curves of solar cells under a given lighting condition is relatively straightforward for production devices, problems begin to arise when making interlab comparisons or when trying to verify a manufacturer's claims regarding the performance parameters of the products they offer. These issues occur because proper (low uncertainty) measurement of the irradiance of the low intensity test light is very challenging. Traditionally, measurements under the standard reporting condition (SRC) with the air mass 1.5 global (AM 1.5 G) spectrum as the reference solar spectrum are performed with a calibrated reference solar cell [21]. Such calibrated reference cells, offered by multiple primary and secondary calibration laboratories around the world, give the short-circuit current, I_{sc}, of the cell under a specific set of illumination and temperature conditions defined by the SRC. The SRC, which has been used by the solar photovoltaic industry for many years, represents one set of possible operating conditions on a clear day [22], [23]. This process almost always involves computation of a spectral correction parameter, which is typically very close to unity when the test and reference cells are of the same material type at the same temperature and/or the test spectrum is very close to the reference spectrum. Not surprisingly, indoor ambient lights differ so much from the SRC conditions that SRC-calibrated reference cells, most of which are Si-based, yield poor measurements of the SRC-equivalent irradiance from indoor ambient light.

At this time, most of the published results for low light performance of solar cells are reported in terms of the illuminance unit, lx (lm/m^2), using an illuminance or lx meter [4], [9], [16], [24], while other researchers have used a scale factor normalized to the sun irradiance to determine the irradiance during their tests [25]. Some very recent standards such as SEMI PV80 [26] have suggested the use of certain historical calorimetry light sources to build an indoor low irradiance simulator, but a calibration service based on an absolute irradiance scale has not yet been established.

Most researchers in the field agree that the use of illuminance without an accompanying spectrum can lead to measurement discrepancies because two different light sources with identical

Manuscript received February 5, 2020; revised March 4, 2020 and May 4, 2020; accepted May 16, 2020. *(Corresponding author: Behrang H. Hamadani.)*

Behrang H. Hamadani is with the National Institute of Standards and Technology (NIST), Gaithersburg, MD 20899 USA (e-mail: behrang.hamadani@nist.gov).

Mark B. Campanelli is with the Intelligent Measurement Systems LLC, Bozeman, MT 59715 USA (e-mail: mark.campanelli@gmail.com).

Color versions of one or more of the figures in this article are available online at https://ieeexplore.ieee.org.

Digital Object Identifier 10.1109/JPHOTOV.2020.2996241

illuminance at the measurement plane can have substantially different spectral and total irradiance output on the solar cell, resulting in different short-circuit currents and *I–V* curves. Therefore, the spectral shape of the light source also needs to be considered. If a relevant reference spectrum is defined and standardized for use under indoor light sources, then interlab measurements can be better facilitated by using the traditional calibrated reference cell method. In this case, all the relevant measurement steps that are currently employed for measurements under the SRC can be translated to low light conditions.

Recently, there have been some efforts to propose a test method or to provide guidelines on how to perform and report the *I–V* curve measurements for an indoor lighting condition, including spectral effects [27]–[29]. In this article, we thoroughly discuss how to extend the traditional reference cell-based method to solar cell measurements under indoor low irradiance conditions. This task was accomplished by constructing multiple reference spectra, appropriate for indoor lighting, and using the absolute spectral responsivity of a given reference cell to calibrate it under the given reference condition. This way, the end user can simply use the reference cell to measure and adjust their setup's light level without needing to know the absolute irradiance of their light source or the absolute quantum efficiencies of their cells or detectors. An important criterion for the choice of a reference cell is the matching of its spectral responsivity to that of the test cell. A spectral correction parameter should be computed and applied to the *I–V* data whenever a spectral mismatch is present.

Since lux-based measurements have already become entrenched in the low-light *I–V* measurement community, we have maintained a connection to them by designing our reference spectra with useful correlated color temperatures (CCT), such that the total illuminance of each spectra equals 1000 lx. The proposed approach significantly streamlines the process of measuring the *I–V* curves under any light irradiance and will allow for the precise computation of the PCE, a determination that is difficult to achieve with low uncertainty given the inherent variability in lux-based measurements. In addition, the proposed methodology facilitates more consistent interlab measurements and comparisons among PV device performances, including the determination of losses.

II. Experimental Details

A dark box was constructed with an opening on its top for in-coupling of a light source. All measurements were performed with two different white LED light sources, projected individually, down onto a stage where both the reference and the test solar cells are placed side by side and under the complete illumination of the LED spotlight. The LEDs are fan-cooled and operated in dc mode with a computer-controlled LED driver having a sourced current resolution of 1 mA. This setup yields a very specific irradiance that can be adjusted to well under 1% of the target *effective irradiance,* as defined below. The setup is such that the irradiance level is first set based on the photocurrent measurements from the reference cell and the simultaneous effective irradiance computation. Then an electronic switch opens up the source meter to the test cell, so that an *I–V* curve sweep can be performed on it, usually from the I_{sc} to the V_{oc}. Fig. 1 shows a photograph of the setup.

The irradiance remains stable to well below 0.1% over the course of the measurement. The light source spectra were measured using an FEL-calibrated spectroradiometer [30] having an uncertainty of about 0.5% in the spectral range of interest.

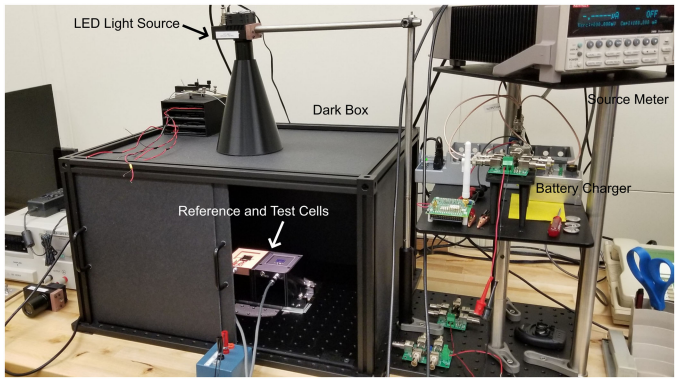

Fig. 1. Experimental testbed used for low-irradiance *I–V* measurements. The reference cell and the test cell are placed next to each on the stage and both cells are equal distance away from the light source.

The differential spectral responsivity (DSR) method was used to calibrate a silicon reference solar cell under the three reference spectra devised for this work. The details of those measurements are published elsewhere [31]–[33]. The linearity of the reference cell under these low irradiance conditions was also investigated [34]. It was determined that this particular reference cell is sufficiently linear (lower than 1% variation) under irradiance levels probed for this work. The expanded uncertainty for this reference cell calibration is estimated at 0.5%.

III. Methodology

Use of a reference solar cell for the measurement of the effective irradiance of the light source during *I–V* measurements of a test device requires acceptance of a reference spectrum and test conditions. This process is usually done in standards committees and can take years to finalize the specifics, including the reference spectrum and the temperature of the test device or its ambient environment. Here, we propose and use three distinct reference conditions for the purpose of demonstrating the measurement and analysis process. Once the reference spectra are defined, the reference solar cell can be calibrated using the DSR method. Then, the combination of the spectral responsivity of the test and the reference cells, along with the spectral irradiance of the reference spectrum and the illuminating source can be used to compute a spectral correction parameter, *M*. The spectral correction parameter can then be used to compute the effective irradiance, *F*, on the test cell for the chosen reference conditions.

A. Reference Spectra

We constructed three reference spectra that are representative of spectral irradiances of commercially available white LEDs. These spectra were adjusted to meet two specific criteria. First, the spectral shape of the light sources was chosen and manually modified, so that they produced three exact CCTs, namely, 3000, 4000, and 6000 K. Second, the illuminance or the luminous flux incident on a surface for each case was set to exactly 1000 lx (lm/m^2). Relative spectral irradiance measurements were performed using a calibrated spectroradiometer on various types of white LEDs and the measured spectra were imported into a CCT calculator to determine each one's color temperature. These spectra were then adjusted, so that the exact CCT numbers listed above were achieved [35]. This task was accomplished iteratively by modifying the ratio between the narrow peak, centered

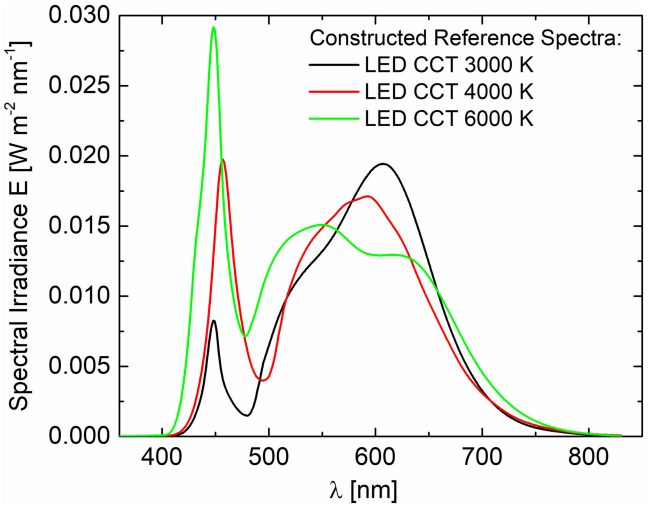

Fig. 2. Three constructed reference spectra used to calibrate a reference solar cell. The illuminance produced by each spectrum is exactly 1000 lx.

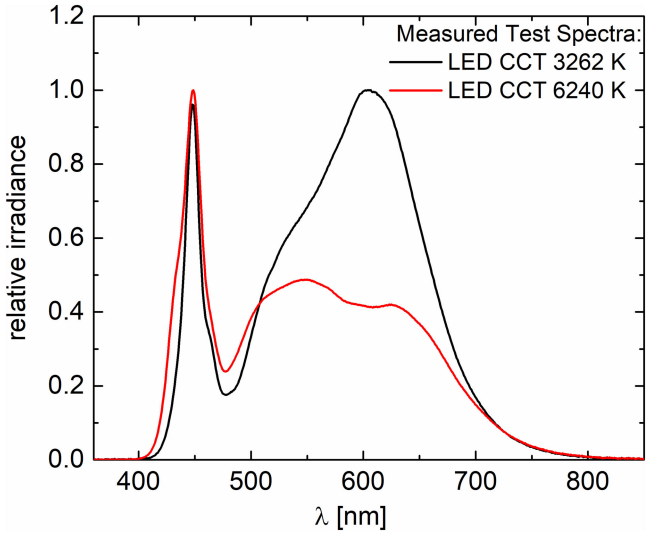

Fig. 3. Relative irradiance plots of two light sources used to perform the *I–V* curve measurements in our setup.

around 450 nm, and the broader peak in the region from 500 to 600 nm. Once the desired color temperatures were achieved, these relative spectral irradiance curves, $\hat{E}$, were scaled by scalar α, so that an absolute spectral irradiance curve $E(\lambda) = \alpha\hat{E}(\lambda)$ for each was computed in SI units of W m^{-2} nm^{-1}

$$E_v = K_m \int_{360\text{ nm}}^{830\text{ nm}} \alpha\hat{E}(\lambda)V(\lambda)d\lambda \qquad (1)$$

where E_v is the illuminance set to 1000 lx, K_m is the spectral luminous efficacy for monochromatic radiation at 555 nm with a value equal to 683 lm/W, and $V(\lambda)$ is the normalized spectral luminous efficiency function, here chosen to be the photopic spectral luminous efficiency function with applications in high light levels such as bright indoor conditions or daylight [36].

Fig. 2 shows a plot of the three reference spectra constructed as described above. Notice that the *y*-axis is in units of spectral irradiance and therefore the total irradiance can be calculated by integrating under each curve. For the reference spectrum with a CCT of 3000 K, the total irradiance, $E_{tot,3k} = 2.9267$ W/m^2; for the 4000 K CCT spectrum, $E_{tot,4k} = 3.1079$ W/m^2; and for the 6000 K CCT spectrum, $E_{tot,6k} = 3.7019$ W/m^2. Clearly, even though all three spectra correspond to an illuminance of 1000 lx–i.e., an average human eye perceives all three as having the same brightness; the radiation power delivered per unit area of the surface is clearly different between the three.

B. Test Spectra

The spectrum of the indoor light source used to evaluate the performance of the PV cells will likely be different from the reference spectra established above. Unlike the reference spectra, which can be synthesized and agreed upon by a standards committee, the test spectra are dependent on each individual light source used to evaluate the devices. Here, we used two different light sources to measure the solar cells. One was a "warm white" LED with a CCT of 3262 K and the other was a "cool white" LED with a CCT of 6240 K. We will show that regardless of the test spectra, one can obtain consistent results for a given reference condition.

Fig. 3 shows relative irradiance plots of the two LED-based indoor light sources used in this work. An absolute irradiance measurement is not needed, but one needs to make sure that the instrument used to measure the spectra is calibrated against a standard lamp, so that the relative shape of the spectra represents the true emission profile of the source. This step is required because the quantum efficiency of solid-state devices used in spectrometers is not constant over such a wide spectral range.

C. Reference Solar Cell Calibrations

A reference solar cell must be chosen and calibrated under the reference conditions. Traditionally, such reference cells are packaged according to the World Photovoltaic Scale (WPVS) recommended design and are calibrated by a national metrology institute (NMI) or a commercial lab with traceability or certification to an NMI scale [37]. Such cells are generally calibrated under the SRC defined by a reference spectrum such as the AM 1.5 G, AM 1.5, or AM 0 (extraterrestrial) spectra and at a given device temperature (typically 25 °C). For the case of measurements under an indoor light source, the use of such reference cells is inappropriate because the spectral composition of the indoor source, angular distribution of the illumination source and the linearity of the reference device itself cannot be easily extrapolated from outdoor conditions, i.e., 1000 W/m^2 of mostly direct sunlight compared with the approximately 3 W/m^2 provided by indoor LED or fluorescent lighting in a mostly diffuse form. Therefore, a reference cell must be calibrated separately for indoor use. Here, we used the DSR method to measure the irradiance spectral responsivity, $R_{r,irr}(\lambda)$ of a linear WPVS silicon reference cell (nominal area 2×2 cm) at 25 °C with light bias provided by the same white LED sources as used for actual performance measurements. Then, the resulting short-circuit current, $I_{r,r}$, under each of the three reference spectra at a temperature of 25 °C is calculated using [31]

$$I_{r,r} = \int_{\lambda\,\min}^{\lambda\,\max} E_r(\lambda)R_{r,\text{irr}}(\lambda)d\lambda \qquad (2)$$

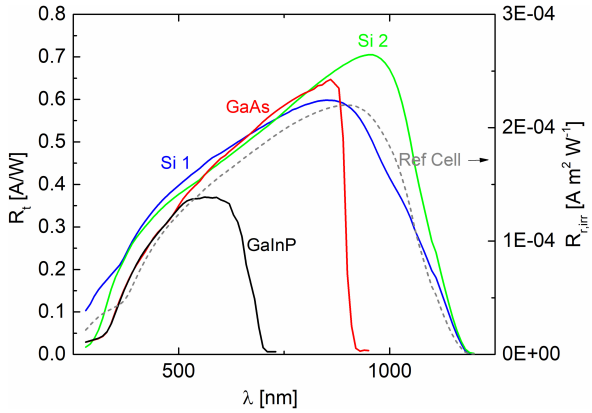

Fig. 4. Power spectral responsivity curves for the four test solar cells measured here. The right axis shows the irradiance spectral responsivity curve for the reference solar cell.

where E_r is the spectral irradiance of a chosen reference spectrum (i.e., one of the three spectra with CCT of 3000, 4000, or 6000 K), and the subscript *r,r* stands for reference cell under reference spectra. The right axis in Fig. 4 shows the irradiance spectral responsivity curve for the reference cell used in these measurements. The integral computation in (2) gives the following calibrated short-circuit currents under each reference spectrum: $I_{r,r}^{CCT3k} = 444.98\ \mu$A, $I_{r,r}^{CCT4k} = 451.47\ \mu$A, and $I_{r,r}^{CCT6k} = 517.70\ \mu$A. These numbers will be used for the computation of the effective irradiance incident on the test cell, depending on the chosen reference conditions.

D. Spectral Responsivity Measurements

Four different types of solar cells were selected and characterized for this study. These devices included two types of silicon solar cells, labeled as "Si 1" and "Si 2," one GaInP solar cell and one GaAs solar cell. Each cell was diced to nominal 2×2 cm dimensions and was mounted inside a 3-D-printed holder fashioned after a WPVS style package with the exception that no glass window was mounted into the holder. The similar geometry of the reference and test cells ensures that variations because of the light source irradiance uniformity or distance from the source are equalized between the two, simplifying computation of any correction factor.

Fig. 4 shows the spectral responsivity curves of the four test cells discussed above in units of A/W. All measurements are based on the DSR technique using a monochromator setup and dc light bias used on each cell. These devices were linear in the irradiance range probed, and the measured spectral responsivity curves are very similar to those reported elsewhere for these types of inorganic semiconductor devices.

E. Spectral Correction Parameter and Effective Irradiance

Given the reference spectral irradiance, the test cell's spectral irradiance (the indoor simulator spectrum) and the spectral responsivities of both the reference and the test solar cells, M can now be calculated [21], [23]

$$M = \frac{\int_{\lambda\,\min}^{\lambda\,\max} R_t(\lambda)E_t(\lambda)\mathrm{d}\lambda \int_{\lambda\,\min}^{\lambda\,\max} R_{r,irr}(\lambda)E_r(\lambda)\mathrm{d}\lambda}{\int_{\lambda\,\min}^{\lambda\,\max} R_t(\lambda)E_r(\lambda)\mathrm{d}\lambda \int_{\lambda\,\min}^{\lambda\,\max} R_{r,irr}(\lambda)E_t(\lambda)\mathrm{d}\lambda} \quad (3)$$

where R_t is the spectral responsivity of the test cell and E_t is the spectral irradiance of the indoor simulator source in relative form. We have assumed that both the reference and the test cells are illuminated by the same light source and that both devices are operated at a temperature of 25 °C. In addition note that the linearity assumption of the short-circuit current with irradiance for both the reference and the test cells are implicit in this computation of *M*.

Recalling that the total irradiance incorporates an underlying spectrum to which the PV devices are sensitive, one can define a unitless effective irradiance, *F*, as the ratio defined by

$$F = \frac{I_{t,t}}{I_{t,r}}, \quad (4)$$

where $I_{t,t}$ is the short-circuit current of the test cell under the testing condition, and $I_{t,r}$ is the short-circuit current of the test cell under the reference condition. The measurement of *F* is readily achieved by monitoring the short-circuit current of a calibrated reference cell mounted in the same plane of irradiance as the test cell. It can be shown [23] that in this case, *F* can be determined by measuring the short-circuit current of the reference cell under the test condition, $I_{r,t}$, relative to the reference cell under the reference condition, $I_{r,r}$, and multiplying by M

$$F = M\frac{I_{r,t}}{I_{r,r}}. \quad (5)$$

An effective irradiance ratio $F = 1$ at the testing plane means that the test device is being exposed to light that produces an equivalent short-circuit current as the reference illumination condition. Oftentimes, $M \neq 1$ and therefore simply adjusting the light levels of the simulator, so that the ratio $I_{r,t}/I_{r,r}$ gives 1 is not sufficient to expose the test cell to the reference condition; so *M* must be computed via (3) and applied instantaneously according to (5), so that *F* is set to a desired level. We also note that if the temperatures of either the test or the reference cells are not at the reference temperature, i.e., $T = 25$ °C, a slight modification to *M* will allow for use of the same formulation given in (5) for determining *F* [23].

F. Current Versus Voltage Curve Measurements Under Reference Conditions

With the goal of measuring the performance of these four types of solar cells under the three reference conditions discussed above, we 1) placed both the reference and the test cells under the illumination source, i.e., indoor solar simulator, 2) calculate the spectral correction parameter *M* for each pair, and 3) adjust the light levels, while simultaneously reading $I_{r,t}$ and calculating *F* using (5) so that $F \rightarrow 1$ as closely as possible. This methodology is accomplished through a computer program that continually monitors the reference cell current output as the drive current I_{LED} sourced to the LED is adjusted. I_{LED} is adjusted in increments of 1 mA, so that the reported *F* is as close to 1 as the resolution of the LED driver allows. In an ideal case where F = 1 is achieved at the test cell irradiance plane, then a 4-probe *I–V* curve is initiated on the test cell from 0 V to the open-circuit voltage, V_{oc}. If *F* is sufficiently close to but not exactly 1, or in cases where the light source is unstable, such that *F* fluctuates during the course of the *I–V* curve sweep, an instantaneous *F* needs to be synchronously monitored and measured along with each (*I*, *V*) data pair. In this case, the *I–V* curve is reported under the reference condition by applying the current-only correction

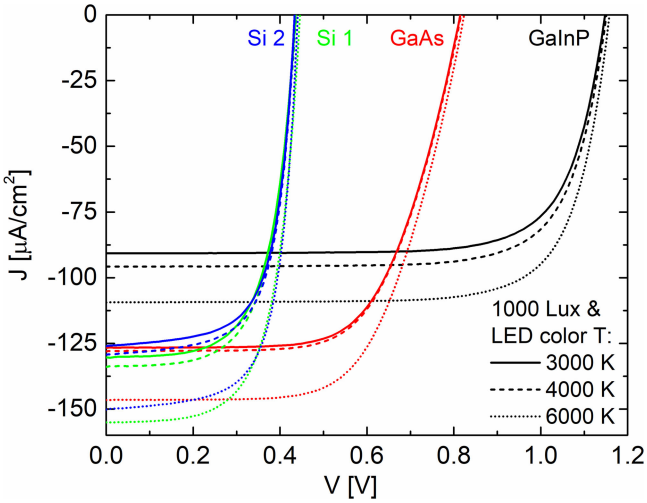

Fig. 5. *I–V* characteristics of the four solar cells measured here, each under a given reference condition as noted in the plot.

[22]

$$I_{t,r}(V) = \frac{1}{M}\frac{I_{r,r}}{I_{r,t}} I_{t,t}(V) = \frac{1}{F} I_{t,t}(V). \tag{6}$$

In case of nonuniformity in the irradiance plane between the reference cell and the test cell (a very common problem under solar simulators and indoor lighting), a nonuniformity correction factor S can be inserted in (6) where S is defined as the ratio $I_{r,\text{ref cell pos}}/I_{r,\text{test cell pos}}$. Usually an average value for I_r in the reference cell position to an average value of I_r in the test cell position is sufficient to calculate S. Therefore, correction (6) can be written as

$$I_{t,r}(V) = \frac{S}{M}\frac{I_{r,r}}{I_{r,t}} I_{t,t}(V) = \frac{S}{F} I_{t,t}(V). \tag{7}$$

IV. Electrical Performance Results

In this work, we report measurement results for the three reference conditions, all having an illuminance of 1000 lx but with different spectral irradiance profiles. As previously discussed, we aimed for $F = 1$ for each of the reference conditions when performing the *I–V* curve sweeps.

Fig. 5 shows three sets of *J–V* curves for each of the four test solar cells described above, where J is the current density obtained by dividing the measured current by the physical area of the cell. For each device, the three curves correspond to one of the three reference conditions. The spectral irradiance of the indoor lighting testbed for the measurements shown in this figure was the 3262 K CCT spectrum (black curve in Fig. 3). Therefore, a spectral correction parameter was calculated for these measurements using this spectrum, the reference spectral irradiance and spectral responsivities of the test and the reference cells as described by (3). This correction parameter was used to obtain the $F = 1$ condition for each curve. It is evident that the device performance is dependent upon the reference condition, even though the illuminance is fixed at 1000 lx under all three settings. This measurement demonstrates that setting up the irradiance with a simple lux meter can lead to significant errors across different types of light sources.

For each of the test cells, it can be seen that the CCT 6000-K reference spectrum produces a higher magnitude J_{sc} and a slightly higher V_{oc} than the 4000 and 3000-K CCT conditions as a result of having a slightly larger total irradiance (≈3.7, 3.1, 2.9 W/m^2, respectively). Table I in the Appendix shows a summary of all the device parameters extracted for all the *I–V* curve measurements on these four solar cells, including additional measurements performed under the CCT 6240-K lighting. M is also shown for each case. It is evident that regardless of the test spectrum used to perform the *I–V* measurement, the device parameters are almost identical under a given reference spectrum as a result of the use of an appropriately computed M in (5) to find the $F = 1$ condition. Even if a very different lighting technology were used for the indoor solar simulator, the *I–V* curve parameters would continue to be the same for a given reference spectra. Further discrepancies could also occur if the directional response of the reference and the test cells are substantially different from each other under mostly diffuse lighting conditions [32], [38].

When the test spectrum has a shape close to that of the reference spectrum, $M \approx 1$ for most of the devices, except for the GaInP cell which has a substantially different spectral responsivity curve than the other three cells. However, when the test spectrum is cool white with a CCT of 6240 K, but the intended reference condition has a CCT of 3000 K, then, even silicon test cells show a mismatch parameter as high as 1.025 for the case "Si1-TS:6240 RS:3k" in Table I. Similar deviations of the mismatch parameter from 1 are seen when the CCT of the reference spectrum differs greatly from that of the test spectrum, as evidenced by the value of M of 0.984 for the case "Si2-TS:3262 RS:6k." These mismatch factors result in approximately a 2% error in the cell's J_{sc} if they were to be ignored. The measurements on the GaInP are also informative. For this cell, M values as high as 1.034 were computed for the "GaInP-TS:6240 RS:3k" case, for example, which is a large error if ignored. An M value substantially different from unity will also have implications on the uncertainty budget of the measurement, a topic that is beyond the scope of this work [39]. In general, the computations in the table show that if a spectral correction parameter is not computed for the measurement, then the potential errors are only minimized if either the indoor simulator's spectrum is chosen to be as close to the reference spectrum as possible, or the test and the reference cells are matched. In photometry language, the test spectrum should be chosen to have a color temperature as close as possible to the reference spectrum's color temperature. If an interlab comparison is being performed when a lux meter is the only available instrument for measurements of light intensity, the two labs should perform the measurements under spectra with similar color temperatures.

A counter-intuitive finding from these measurements is that under the CCT 6000-K spectrum, the power conversion efficiency is actually reduced for all four cases. The GaInP cell shows a PCE of ≈26.8% under a 3000-K, (1000 lx) spectrum but shows a reduced PCE of ≈25.9% under the 6000-K spectrum. Similarly, the GaAs cell's PCE drops from 22.8% under the 3000-K spectrum to 20.6% under the 6000-K spectrum. Similar smaller reductions in PCE are observed in the two silicon cells. This finding is in spite of the fact that the electrical performance parameters, including the maximum power point, P_m, are actually higher under the 6000-K spectrum than under the 3000-K spectrum for all cells. The efficiency, which is the ratio of the

output power to input power, sees a reduction at higher CCT spectra because the boost in mostly $J_{\rm sc}$ and J_m (the max power point) is not sufficient to raise the P_m high enough, so that it can result in an increase in the PCE. The higher CCT spectra pack more of their optical power in the 400 to 500-nm regime, but the solar cells have lower spectral responsivities in that regime and are unable to tap into this extra power efficiently; therefore, they show a reduction in power conversion efficiency. This finding is consistent with other results in the literature. For example, the record PCE of 28.9% for a dye-sensitized cell at 1000 lx reported in Freitag *et al.* was measured under warm-white fluorescent lighting [8]. The same cell under a cooler color temperature will likely show a PCE lower than this value.

From among these four cells, the GaInP cell outperforms the other cells by a significant margin. Interestingly, the GaInP cell also shows a much higher fill factor, 75%, than the others, likely a result of lower series resistance and/or a higher shunt resistance and lower nonradiative recombination losses. It shows a PCE that is more than 10 percentage points higher than its 1-sun performance (≈15%, data not shown versus 26.8% here) because of the near perfect match between its spectral responsivity and the white LED spectra. On the other hand, the GaAs devices showed a PCE comparable or slightly lower than their 1-sun performance.

Finally, we draw attention to the performance parameters of the two silicon cells measured here. Under the 3000-K CCT reference spectrum, one cell (Si1) produces 3.5% more light generated current per unit area than the other, delivering a respectable PCE of 12.5% (≈19.9%, under the SRC, not shown) However, Si2 also gives a similar PCE, making up for the lower $J_{\rm sc}$ by having a slightly higher FF. Therefore, even silicon, when optimized, can be utilized under low light conditions, particularly if natural sunlight is mixed in with the artificial light as that will increase the PCE.

V. Conclusion

We have laid out a foundation for performing low-irradiance *I–V* curve measurements for PV devices intended for use under indoor ambient lighting based on the use of a reference solar cell calibrated under a carefully chosen reference irradiance. We devised various versions of this reference spectrum, with a focus on changing its photometric color temperature, while still keeping its total illuminance at 1000 lx, so that we can clearly measure the effect of these changes on the performance parameters of four different types of solar cells. Our results confirm a foregone conclusion in the research community that the spectral composition of the light source does indeed affect the performance of the solar cells. Our methodology and measurement approach clearly explain why this dependence is the case and lead the way to develop standards to deal with these measurement challenges.

Appendix

Please see Table 1.

Acknowledgment

Behrang H. Hamadani would like to thank C. Miller of NIST for providing the CCT computational worksheet, J. Roller of NIST for programming and automating the measurement instruments used in this work, Y.-T. Li of ITRI for providing some of the silicon cells used in these measurements, and H. Yoon of NIST for discussions and various collaborative work.

TABLE I
I–V Curve Measurement Parameters for the Four Solar Cells Under Two Different Test Spectra and Three Different Reference Conditions

Device/Condition	V_{oc} (V)	J_{sc}(μA/cm^2)	V_m (V)	J_m (μA/cm^2)	FF	P_m (μW/cm^2)	*M*	% PCE
GaAs-TS:3262 RS:3k	0.815	126.7	0.590	113.2	0.647	66.8	0.998	22.82
GaAs-TS:6240 RS:3k	0.816	127.1	0.590	113.4	0.645	66.9	0.995	22.85
GaAs-TS:3262 RS:4k	0.816	128.0	0.590	114.1	0.644	67.3	1.002	21.67
GaAs-TS:6240 RS:4k	0.817	128.5	0.590	114.4	0.643	67.5	0.999	21.72
GaAs-TS:3262 RS:6k	0.824	146.6	0.580	131.3	0.630	76.1	1.003	20.56
GaAs-TS:6240 RS:6k	0.824	147.1	0.580	131.6	0.630	76.3	1.000	20.62
GaInP-TS:3262 RS:3k	1.148	90.8	0.960	81.6	0.752	78.3	1.018	26.76
GaInP-TS:6240 RS:3k	1.149	91.0	0.950	82.5	0.750	78.4	1.034	26.77
GaInP-TS:3262 RS:4k	1.151	95.8	0.960	86.5	0.753	83.0	0.978	26.71
GaInP-TS:6240 RS:4k	1.152	96.1	0.950	87.5	0.751	83.2	0.993	26.76
GaInP-TS:3262 RS:6k	1.158	109.4	0.960	99.9	0.757	95.9	0.983	25.91
GaInP-TS:6240 RS:6k	1.159	109.8	0.960	100.1	0.755	96.1	0.998	25.96
Si1-TS:3262 RS:3k	0.436	130.4	0.330	110.8	0.643	36.6	1.008	12.49
Si1-TS:6240 RS:3k	0.437	130.2	0.330	110.8	0.643	36.6	1.025	12.50
Si1-TS:3262 RS:4k	0.437	134.0	0.330	114.1	0.643	37.6	0.995	12.11
Si1-TS:6240 RS:4k	0.439	133.8	0.330	114.6	0.644	37.8	1.012	12.17
Si1-TS:3262 RS:6k	0.446	155.1	0.340	132.2	0.650	45.0	0.984	12.15
Si1-TS:6240 RS:6k	0.447	154.9	0.340	132.5	0.651	45.1	1.001	12.17
Si2-TS:3262 RS:3k	0.434	126.0	0.340	107.8	0.670	36.6	1.008	12.52
Si2-TS:6240 RS:3k	0.433	126.1	0.340	106.8	0.665	36.3	1.025	12.41
Si2-TS:3262 RS:4k	0.434	129.3	0.340	110.4	0.668	37.5	0.996	12.07
Si2-TS:6240 RS:4k	0.434	129.4	0.340	109.6	0.664	37.3	1.013	11.99
Si2-TS:3262 RS:6k	0.441	150.2	0.350	128.6	0.680	45.0	0.984	12.16
Si2-TS:6240 RS:6k	0.440	150.2	0.350	128.0	0.677	44.8	1.001	12.10

Naming convention for each device/condition provides the device as described in Section III-D, the CCT of the test spectrum (TS), and the CCT of the reference spectrum (RS).

REFERENCES

[1] J. A. Paradiso and T. Starner, "Energy scavenging for mobile and wireless electronics," *IEEE Pervasive Comput*., vol. 4, no. 1, pp. 18–27, Jan. 2005.

[2] R. Haight, W. Haensch, and D. Friedman, "Solar-powering the Internet of Things," *Science*, vol. 353, no. 6295, pp. 124–125, Jul. 2016.

[3] A. Nasiri, S. A. Zabalawi, and G. Mandic, "Indoor power harvesting using photovoltaic cells for low-power applications," *IEEE Trans. Ind. Electron.*, vol. 56, no. 11, pp. 4502–4509, Nov. 2009.

[4] M. Masoudinejad *et al.*, "Development of a measurement platform for indoor photovoltaic energy harvesting in materials handling applications," in *Proc. 6th Int. Renewable Energy Congr.*, 2015, pp. 1–6.

[5] H. Shao, C. Tsui, and W.-H. Ki, "The design of a micro power management system for applications using photovoltaic cells with the maximum output power control," *IEEE Trans. Very Large Scale Integration Syst.*, vol. 17, no. 8, pp. 1138–1142, Aug. 2009.

[6] M. Freunek, M. Freunek, and L. M. Reindl, "Maximum efficiencies of indoor photovoltaic devices," *IEEE J. Photovolt.*, vol. 3, no. 1, pp. 59–64, Jan. 2013.

[7] N. H. Reich, W. G. J. H. M. van Sark, and W. C. Turkenburg, "Charge yield potential of indoor-operated solar cells incorporated into product integrated photovoltaic (PIPV)," *Renew. Energy*, vol. 36, no. 2, pp. 642–647, Feb. 2011.

[8] M. Freitag *et al.*, "Dye-sensitized solar cells for efficient power generation under ambient lighting," *Nature Photon.*, vol. 11, no. 6, pp. 372–378, Jun. 2017.

[9] P. Vincent *et al.*, "Indoor-type photovoltaics with organic solar cells through optimal design," *Dyes Pigments*, vol. 159, pp. 306–313, Dec. 2018.

[10] H. K. H. Lee *et al.*, "Organic photovoltaic cells – promising indoor light harvesters for self-sustainable electronics," *J. Mater. Chem. A*, vol. 6, no. 14, pp. 5618–5626, 2018.

[11] Y. Aoki, "Photovoltaic performance of organic photovoltaics for indoor energy harvester," *Organic. Electronics*, vol. 48, pp. 194–197, Sep. 2017.

[12] S. Park *et al.*, "Self-powered ultra-flexible electronics via nano-grating-patterned organic photovoltaics," *Nature*, vol. 561, no. 7724, pp. 516–521, Sep. 2018.

[13] J. Dagar, S. Castro-Hermosa, G. Lucarelli, F. Cacialli, and T. M. Brown, "Highly efficient perovskite solar cells for light harvesting under indoor illumination via solution processed SnO_2/MgO composite electron transport layers," *Nano Energy*, vol. 49, pp. 290–299, Jul. 2018.

[14] K. A. Haque and M. Z. Baten, "On the prospect of CZTSSe-based thin film solar cells for indoor photovoltaic applications: A simulation study," *AIP Advances*, vol. 9, no. 5, May 2019, Art. no. 055326.

[15] I. Mathews, G. Kelly, P. J. King, and R. Frizzell, "GaAs solar cells for indoor light harvesting," in *Proc. IEEE 40th Photovolt. Specialist Conf.*, 2014, pp. 0510–0513.

[16] I. Mathews, P. J. King, F. Stafford, and R. Frizzell, "Performance of III–V solar cells as indoor light energy harvesters," *IEEE J. Photovolt.*, vol. 6, no. 1, pp. 230–235, Jan. 2016.

[17] A. S. Teran *et al.*, "Energy harvesting for GaAs photovoltaics under low-flux indoor lighting conditions," *IEEE Trans. Electron Devices*, vol. 63, no. 7, pp. 2820–2825, Jul. 2016.

[18] V. Bahrami-Yekta and T. Tiedje, "Limiting efficiency of indoor silicon photovoltaic devices," *Opt. Express*, vol. 26, no. 22, pp. 28238–28248, Oct. 2018.

[19] Y. Afsar, J. Sarik, M. Gorlatova, G. Zussman, and I. Kymissis, "Evaluating photovoltaic performance indoors," in *Proc. 38th IEEE Photovolt. Specialists Conf.*, 2012, pp. 001948–001951.

[20] G. Bunea, K. Wilson, Y. Meydbray, M. Campbell, and D. De Ceuster, "Low light performance of mono-crystalline silicon solar cells," in *Proc. IEEE 4th World Conf. Photovolt. Energy Conf.*, vol. 2, 2006, pp. 1312–1314.

[21] K. Emery and C. Osterwald, "Measurement of photovoltaic device current as a function of voltage, temperature, intensity and spectrum," *Sol. Cells*, vol. 21, no. 1/4, pp. 313–327, Jun. 1987.

[22] *Standard Test Method for Electrical Performance of Photovoltaic Cells Using Reference Cells Under Simulated Sunlight*, ASTM Standard E948-16, ASTM International, West Conshohocken, PA, USA, 2016.

[23] M. B. Campanelli and B. H. Hamadani, "Calibration of a single-diode performance model without a short-circuit temperature coefficient," *Energy Sci. Eng.*, vol. 6, no. 4, pp. 222–238, Aug. 2018.

[24] M. Rasheduzzaman, P. B. Pillai, A. N. C. Mendoza, and M. M. De Souza, "A study of the performance of solar cells for indoor autonomous wireless sensors," in *Proc. 10th Int. Symp. Commun. Syst., Netw. Digit. Signal Process.*, 2016, pp. 1–6.

[25] J. Russo, W. Ray, and M. S. Litz, "Low light illumination study on commercially available homojunction photovoltaic cells," *Appl. Energy*, vol. 191, pp. 10–21, Apr. 2017.

[26] Specification of indoor lighting simulator requirements for emerging photovoltaic, SEMI PV80-0218, Milpitas, CA, USA, 2018.

[27] B. Minnaert and P. Veelaert, "A proposal for typical artificial light sources for the characterization of indoor photovoltaic applications," *Energies*, vol. 7, no. 3, pp. 1500–1516, Mar. 2014.

[28] X. Ma, S. Bader, and B. Oelmann, "Characterization of indoor light conditions by light source classification," *IEEE Sensors J.*, vol. 17, no. 12, pp. 3884–3891, Jun. 2017.

[29] J. F. Randall and J. Jacot, "Is AM1.5 applicable in practice? Modelling eight photovoltaic materials with respect to light intensity and two spectra," *Renewable Energy*, vol. 28, no. 12, pp. 1851–1864, Oct. 2003.

[30] H. W. Yoon and C. Gibson, "Spectral irradiance calibrations," Nat. Inst. Standards Technol., Gaithersburg, MD, USA, NIST Spec. Publ. 250-89, 2011.

[31] J. Roller and B. H. Hamadani, "Reconciling LED and monochromator-based measurements of spectral responsivity in solar cells," *Appl. Opt.*, vol. 58, no. 22, Aug. 2019, Art. no. 6173.

[32] B. H. Hamadani, J. Roller, A. M. Shore, B. Dougherty, and H. W. Yoon, "Large-area irradiance-mode spectral response measurements of solar cells by a light-emitting, diode-based integrating sphere source," *Appl. Opt.*, vol. 53, no. 16, Jun. 2014, Art. no. 3565.

[33] B. H. Hamadani, J. Roller, B. Dougherty, F. Persaud, and H. W. Yoon, "Absolute spectral responsivity measurements of solar cells by a hybrid optical technique," *Appl. Opt.*, vol. 52, no. 21, Jul. 2013, Art. no. 5184.

[34] B. H. Hamadani, A. Shore, J. Roller, H. W. Yoon, and M. Campanelli, "Non-linearity measurements of solar cells with an LED-based combinatorial flux addition method," *Metrologia*, vol. 53, no. 1, pp. 76–85, Feb. 2016.

[35] C. C. Miller, Y. Zong, and Y. Ohno, "LED photometric calibrations at the national institute of standards and technology and future measurement needs of LEDs," in *Proc. SPIE4th Int. Conf. Solid State Lighting*, vol. 5530, 2004, pp. 69–79.

[36] T. M. Goodman *et al.*, "The use of terms and units in photometry - implementation of the CIE system for mesopic photometry," International Commission on Illumination, Vienna, Austria, CIE TN004, 2016.

[37] C. R. Osterwald *et al.*, "The world photovoltaic scale: An international reference cell calibration program," *Prog. Photovolt.*, vol. 7, no. 4, pp. 287–297, Jul. 1999.

[38] S. Winter, D. Friedrich, and T. Gerloff, "Effect of the angle dependence of solar cells on the results of indoor and outdoor calibrations," in *Proc. 25th Eur. Photovoltaic Sol. Energy Conf Exhib.*, 2010, pp. 4304–4306.

[39] H. Field and K. Emery, "An uncertainty analysis of the spectral correction factor," in *Proc. Conf. Record 23rd IEEE Photovolt. Specialists Conf.*, 1993, pp. 1180–1187.

Behrang H. Hamadani received the B.S. degree in physics from University of Texas at Dallas, TX, USA, in 2001, and the Ph.D. degree in physics from Rice University, Houston, TX, USA, in 2007.

He is a Project Leader with the National Institute of Standards and Technology, Gaithersburg, MD, USA. His research interests include electronic and opto-electronic measurements and characterization of solar cells and he has developed a variety of novel techniques to study the physics of solar cells. He's also developed calibrated reference solar cells directly traceable to fundamental SI units.

Dr. Hamadani received the Presidential Early Career Award for Scientists and Engineers, in 2019.

Mark B. Campanelli received the Ph.D. degree in mathematics from Montana State University, Bozeman, MT, USA, in 2009.

He is the owner of Intelligent Measurement Systems LLC in Bozeman, MT, USA. His current work focuses on developing user-friendly software at the nexus of current-voltage measurements and the calibration of physics-based lumped-parameter photovoltaic performance models. For more information please visit https://intelligentmeasurementsystems.com/